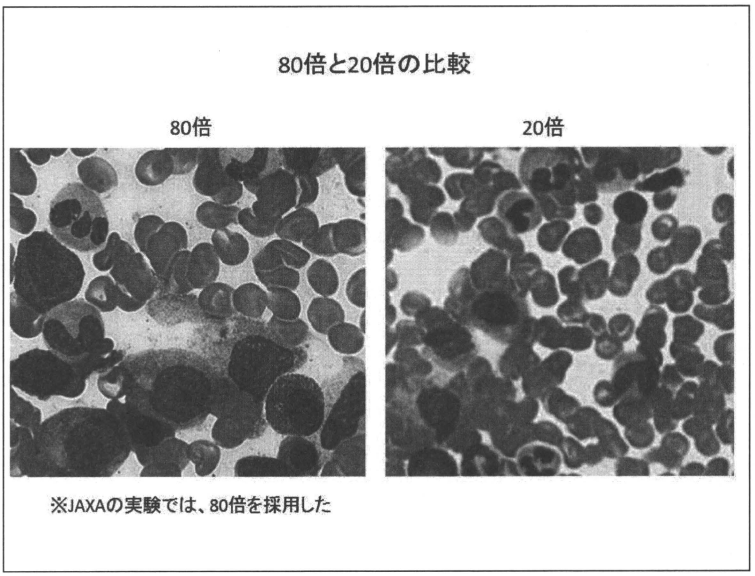

図 1

厚生労働科学研究費補助金（がん臨床研究事業）
分担研究報告書

バーチャルスライドを用いた医学教育・研究・病理診断に関する研究

研究分担者　井藤 久雄　　鳥取大学医学部医学科　教授

研究要旨

バーチャルスライド(VS)の医学教育・研究・病理診断への応用について研究した。

1．医学学生の病理組織実習に用いたところ、学生の 95%が顕微鏡よりも VS の方が効率的と回答した。

2．三カ国をむすび卵巣癌 331 症例の病理組織診断の妥当性を 16 名の病理医が VS にて検討した。効率よく検討が進み、12 例(3.6%)が除外された。

3．VS を使用した術中迅速診断 175 例と過去に静止画像ないしセミ動画で実施された 932 例について比較した。正診率は前者で 97.7%、後者で 97.5%であり差はなかった。病理組織診断に必要な時間は各々 4 分以内、2〜44 分であった。VS では視野と倍率を病理医が選択可能なことから心理的負担は大幅に軽減された。

4．435 例のパラフィン包埋生検標本を VS にて診断した。311 例は消化管生検であり、71.5%を占めていた。直接検鏡との比較で正診率は 98.4%であった。移植臓器生検標本を VS で診断したが、生診率や画像の質に置いて直接検鏡との差はなかった。

A.研究目的

医学教育や研究分野でのバーチャルスライド(VS)応用が始まっている。また、がん診療連携拠点病院においても病理医が不足している現在、VS を用いた病理診断の有用性が期待されている。しかし、VS の導入・応用については病理医数や地域性により医療機関の対応が異なる。本研究では、改めて VS による病理診断の有用性を検討した。

B.研究方法

病理組織実習を行っている鳥取大学医学部医学科 2 年生 83 名に VS に関するアンケート調査を無記名、自由記載方式で行った。

婦人科悪性腫瘍化学療法研究機構(Japanese Gynecologic Oncology Group; JGOG)が実施する共同研究「卵巣明細胞癌」の病理診断を VS を用いて再評価した。卵巣明細胞癌 331 例のスライドを Web にアップロード、3 カ国の病理医が事前に診断して、疑問例を同一画像を観察しつつ検討した。

鳥取大学附属病院から東約 50km に位置している鳥取県立厚生病院(304 床、地域がん診療連携拠点病院、常勤病理医不在)と実施している遠隔病理診断の精度や問題点について検証した。附属病院から週 1 回、病理医を派遣しているが、術中迅速診断を日常的に実施することは出来ない。そこで、2008 年 4 月から VS を用いた術中迅速診断を開始した。数日以内に郵送されたスライドを直接検鏡して、診断を確認した。

さらに、移植病理に精通している病理医は稀であり、移植臓器病理診断における BS の有用性をこれまでに保管されているスライド標本を用いて検討した。

なお、用いたシステムはオリンパス社製 VS100 OlyVIA(Ver.2.1)であり、鳥取県情報ハイウエー（光ファイバー）で接続した。

（倫理面への配慮）

学生実習標本ならびにJGOGのカンファレンスに使用したスライドは連結不可能匿名化して使用し

た。遠隔病理診断に関しては鳥取大学医学部倫理委員会に申請して、承認を受けた。

C.研究結果

1. 病理組織実習への利用に関するアンケート調査

83名中79名(95.2%)が顕微鏡よりもVSが利用しやすいと答えた。その理由として、目が疲れない、操作が簡単、視野が広い、教員に質問しやすい、学生同士で相談しやすいなどを挙げた。他方、3名はどちらとも言えない、と答えた。その理由として、顕微鏡のほうが記憶に残りやすい、VS は立体的でない、将来、顕微鏡が使えないと不便、と記載していた。なお、23名は学外（自宅）での観察を希望していた。

2. バーチャルスライド（VS）を用いた婦人科悪性腫瘍病理診断の評価

鳥取大学に4人、北里大学に9人、英国グラスゴー大学1名、Pascale国立がんセンター（イタリア）2人の計16人の病理医が参加した。2名以上の病理医が「不適格の可能性有り」、「判定困難」として症例について同一画面を観察しつつ、討論した。検討は円滑に進み12例(3.6%)がエントリー保留とされた。

3. VS を利用した病理診断の運用；静止画、セミ動画との対比

2010 年 12 月まで 175 症例が VS を用いて術迅速診断が実施されていた。その内訳は肺・縦隔腫瘍 80 病変、脳神経領域 27 病変、肝胆道系 22 病変、乳腺腫瘍 23 病変、甲状腺腫瘍 6 病変、卵巣腫瘍 6 病変、その他 11 病変であった。標本作製と画像取り込みは 7〜10 分、診断はすべて 4 分以内で完了していた。VS 導入以前に実施していた静止画やセミ動画で診断した 932 例では病理診断は 2〜44 分であった。正診率は前者で 97.7%、後者で 97.5%であり両群間で差はなかった。

2010 年 10 月までの 2 年 10 ヵ月で 435 例のパラフィン包埋生検標本を VS にて診断していた。311 例は消化管生検であり、71.5%を占めていた。直接検鏡との比較で正診率は 98.4%であった。

4．VS による移植臓器生検診断

過去に診断されていた移植腎生検 4 例、移植肝生検 2 例を VS に取り込み、鳥取大学医学部にて検鏡した。VS 診断は通常の検鏡診断と等質性を有していた。

D.考察

VSの用途は多種多様であり、医学教育の現場では導入している医育機関が少なくない。特に、顕微鏡実習に関してはスライド標本を学生数だけ用意する必要がない、同一画面での指導、ディスカッションが容易である等の利点が多い。学生教育の場ではZ軸の必要性は低い。今後は授業のみならず、自己学習においてもVSの利用が展開されよう。

JGOGの共同研究として「卵巣明細胞癌」の病理診断をVSを用いて三カ国16人の病理医が再評価した。2名以上の病理医が「不適格の可能性有り」、「判定困難」として症例について同一画面を観察しつつ、討論したが、検討は円滑に進み12例がエントリー保留とされた。時間と距離を超えたミーティングであり、VSの大きな利点と見なされる。今後もこうした試みが日常的に実施されよう。

病理組織診断に関しては、特に術中迅速診断への応用が開始されている。2010 年度に日本医師会が 2,606 病院に対して診療科別の不足医師数を調査した。病院医師で必要とされている医師は病理医が 377 人で最多であった(社団法人 日本医師会定例記者会見、2010 年 10 月 6 日)。因みに、婦人科 291 人、救急医 207 人、リハビリ 199 人である。鳥取県ではがん診療連拠点病院 4 病院中、県立厚生病院を含む 2 病院で常勤病理医が不在である。VS による術中迅速診断ががん診療連携拠点病院の機能を補っており、執刀医からも好評である。

興味あることに術中迅速診断の正診率は静止画・セミ動 画と VS の何れも約 98%である。しかし、VS では検体提出から 30 分以内には術者に伝達され、大幅に短縮された。さらに、数値化は出来ないが、病理医の心理的負担は著しく軽減した。診断側病理医が観察視野と倍率を選択できる利点が大きい。

VS を用いた病理診断は通常のパラフィン包埋標本でも実施されている。診断精度に関しては通常の検鏡と変わらない。このことは移植臓器生検標本の

VS 診断でも確認された。VS を用いた病理診断の利点は、アップロードされた画像を、病理医は時間的余裕のある時に診断すればよいことにある。従って、VS は病理組織診断のコンサルテーションには最適である。今後、病理組織診断に関しては直接検鏡と VS が両輪となる可能性が示唆された。

E.結論

VS を用いた遠隔病理診断は直接検鏡と同等の診断精度を有し、しかも、距離のバリアーがないので病理医不在の医療機関でも術中迅速診断が可能である。今後、病理診断のみならず、医学教育や研究の領域でも VS の利用は広まるものと見なされる。

F.健康危険情報

なし

G.研究発表

1.論文発表

なし

2.学会発表

1. 紙谷秀樹、石橋美名子、堀江　靖、井藤久雄：脳腫瘍手術時バーチャルスライドシステムによる術中迅速病理診断の活用．日本脳腫瘍病理学会．2010 年 5 月 21 日．大阪．

2. 紙谷秀樹、石橋美名子、堀江　靖、井藤久雄：脳腫瘍手術時バーチャルスライドシステムによる術中迅速病理診断の活用．鳥取県春期医学会．2010 年 6 月 6 日．倉吉．

H.知的財産権の出願・登録状況（予定を含む）

1. 特許取得

なし

2. 実用新案登録

なし

3. その他

なし

バーチャルスライドを用いた遠隔病理診断の実践

2011年2月10日

テレパソロジーの応用

1．術中迅速診断

＊静止画：2007年3月6日現在　932臓器

正診率＝正診数＋許容診断数／全臓器数＝864＋45／932＝97.5%

① 庄原赤十字病院：静止画＋動画(ISDN4回線)

② 倉吉厚生病院：静止画

＊Virtual Slide：2007年12月　2010年12月

倉吉厚生病院　175例

2．細胞診断

3．移植臓器病理生検診断

4．学生教育および学内カンファレンス

- 一般300床 感染症（第一種）2床（第二種）2床
- 病理組織　約１８００件/年
- 病理医　週２回来院　（木曜日・金曜日）
- テレパソロジー（遠隔病理診断）

1997年～　：電話回線を用いた静止画
術中迅速病理診断

2007年12月～：バーチャルスライドを導入
術中迅速病理診断
生検組織診断（一部）

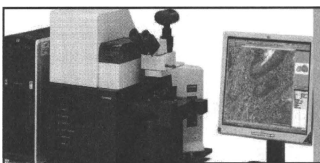

バーチャルスライドシステム
VS-100

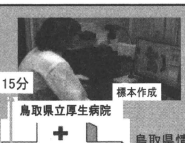

30分以内に
診断情報が判明

15分

標本作成

7分以内
（標本作製＋画像取り込み）

鳥取県立厚生病院

鳥取大学医学部

鳥取県情報ハイウェイ

50Km

手術

診断病理医

5分

術中迅速組織診断件数

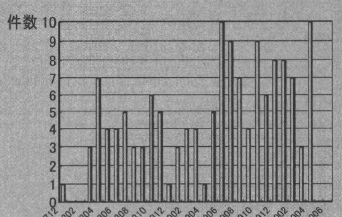

VSを用いた術中迅速診断

鳥取県立厚生病院 (2007年12月　2010年12月)

病変	症例数
肺・縦隔病変	80
脳神経領域	27
乳腺腫瘍	23
肝胆道系病変	22
甲状腺腫瘍	6
卵巣腫瘍	6
その他	11

正診率＝正診数＋許容診断数／全臓器数＝171／175＝97.7%

術中Virtual Slide Telepatholgy施行した症例の結果

Case	Sex	Age	Tumor Localization	Pre-operative Diagnosis	Rapid Pathological Diagnosis by Virtual Slide Telepathology	Final Pathological Diagnosis	Effectiveness by Rapid Pathological Diagnosis
1	M	66	Rt. Frontal skull	Metastasis	Metastatic brain tumor	Metastatic Tumor from Bladder Carcinoma	
2	F	53	Rt. Frontal	Convexity meningioma	Meningioma	Meningotheliomatous Meningioma	
3	F	60	Rt. Frontal	Resurrent anaplastic astrocytoma	Malignant Astrocytoma	Anaplastic Astrocytoma	
4	F	43	Rt. Frontal base	Cavernous angioma	Angioma	Cavernous Angioma	
5	F	18	Rt. Frontal	Malignant glioma or Germ cell tumor	Germinoma	Germinoma with STGC	○
6	F	42	Rt. Frontal skull	Osteoma	Osteoma	Osteoma	
7	M	22	Lt. Thalamus	Malignant glioma or Malignant lymphoma	Malignant Astrocytoma	Anaplastic Astrocytoma	○
8	F	70	Pineal area	Recurrent glioblastoma	Malignant Astrocytoma	Glioblastoma	
9	F	12	Lumbar spinal	Medulloblastoma	Medulloblastoma	Medulloblastoma	
10	M	14	Pineal area	Germ cell tumor	Germinoma	Pure Germinoma	
11	F	59	Rt. frontal	Convexity meningioma	Meningioma	Meningotheliomatous Meningioma	
12	M	68	Rt. parietal	Malignant glioma	Malignant glioma	Anaplastic Oligo-astrocytoma	
13	M	67	Cellebellum	Metastasis	Adenocarcinoma	Metastatic Adenocarcinoma from Lung	
14	M	78	Lt. Occipital	Metastasis	Undetermined	Metastatic Adenocarcinoma from Lung	
15	M	54	Cellebellum	Metastasis	Meta Small cell carcinoma in PNET like	Small Cell Carcinoma from Lung	
16	M	61	Lt. CP angle	Vestibular neurinoma	Neurinoma	Neurinoma	
17	F	73	Lt. Frontal ~ corpus callosum	Glioblastoma	Malignant Astrocytoma	Anaplastic Astrocytoma	
18	M	66	Rt. Frontal	Convexity meningioma	Meningioma	Transitional Type Meningioma	
19	M	73	Rt. Occipital	Metastasis	No tumor	Radiation Necrosis	

症例　58歳　男性　頭痛

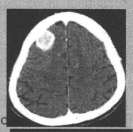

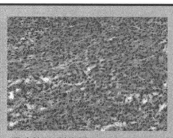

迅速診断：髄膜腫（Whorling pattern あり）

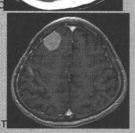

Gd-T

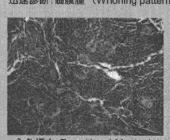

永久標本：Transitional Meningioma

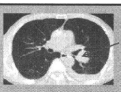

BFにて
診断つかず

左肺門部腫瘍(+)

症例　54歳　男性
歩行障害

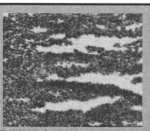

迅速診断：転移ならsmall cell carcinoma
原発なら　PNET　like

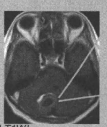

Gd-T1WI

永久標本：転移　small cell carcinoma

生検組織診断の運用方法

目的：再来予約日にあわせての迅速な結果報告

ホルマリン固定検体をパラフィン標本作製
⇒VS-100にて画像取込み⇒サーバーへ保存する
⇒依頼書をFAXにて送信する
⇒病理医は都合のいい時間に閲覧し、診断する
⇒FAXにて、報告書を受信する
⇒一次報告（報告書をスキャナーする）
⇒後日、直接鏡検診断結果を最終報告とする

生検組織診断

期間：2007年12月～2010年4月
生検組織診断　435件

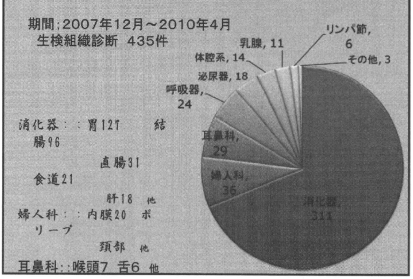

バーチャル診断と直接鏡検診断

診断不一致事例	件数
VS診断とパラフィン標本と診断が異なった	7
パラフィン標本を深切りして診断が異なった	6
パラフィン標本で免疫染色にて最終診断	5
生検標本で特殊染色、免疫染色にて最終診断	16
生検標本で直接鏡検にて最終診断	2

正診率＝４２８÷４３５＝９８．４％

＊日本医療マネジメント学会、
第7回鳥取支部学集会：パネルディスカッション
「地域医療連携におけるITの活用－
地域医療再生のためのITネットワーク」
病理診断とテレパソロジー

鳥取県立厚生病院中央検査室　岡田早苗

＊第28回日本脳腫瘍病理学会 2010（大阪）
バーチャルスライドシステムによる
遠隔地術中脳腫瘍病理診断の活用

鳥取県立厚生病院脳神経外科 紙谷秀規

まとめ

＊静止画、セミ動画とＶＳで術中迅速診断の正診率に差はない。
９７．５％ vs ９７．７％

＊診断時間は明らかに短縮：
２　４４分 vs １　４分

＊診断の心理的負担は明らかに軽減

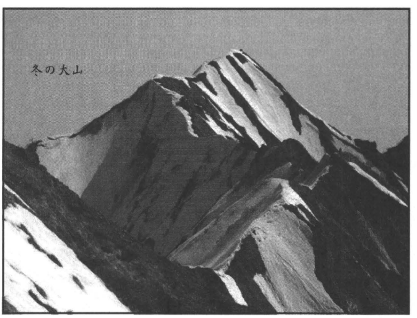

厚生労働科学研究費補助金（がん臨床研究事業）
分担研究報告書

バーチャルスライドを用いた皮膚腫瘍性病変の学習ツールの試み

研究分担者　猪山 賢一　　熊本大学・医学部附属病院・病理部　准教授
研究協力者　本田 由美　　熊本大学・医学部附属病院・病理部　助教

研究要旨

実践的病理学教育には病変の場のマクロおよびミクロレベルの膨大かつ詳細な知識を医学部学生ないし有能な臨床医師の養成に不可欠である。近年、バーチャルスライドの進歩と普及とともに、医学部病理学講義および病理組織学の実習においてもバーチャルスライドが導入されつつある。本研究では医学部学生に対し皮膚腫瘍性病変の病理組織像に関してバーチャルスライドを用いて講義を行い、その学習ツールとしての利点と問題点を検討した。利点としては従来のスライド投影の講義方式に比較してより詳細に視覚に訴える事ができ、病変部以外と対比させながら病変の全体像を理解させる事ができた。問題点としては画像データの容量が大きく、スキャンやデータ整理などの準備に手間がかかった。限られた講義時間内で要領良く提示する為に必要最小限の範囲を効率良くスキャンする必要があり、講義者自らがスキャンする必要があった。これらの問題点が改善されていけば、バーチャルスライドが学習ツールとして大きく発展することが期待された。

A.研究目的

臨床医の育成には実践的病理学教育が不可欠である。近年、バーチャルスライド技術の急速な進歩とともに、医学部病理学講義および実習においてもバーチャルスライドの導入が実施されつつある。本研究では医学部学生に対する病理学各論の講義の中で皮膚腫瘍性病変に関してバーチャルスライドでの講義を行い、その利点と問題点に関して検討した。

B.研究方法

バーチャルスライドは OLYMPUS VS=100 を用いた。サーバー容量：4.8TB(バックアップ保存領域 2.4TB, RAID5)を用いた。病理部保存の皮膚腫瘍性病変とウイルス感染症に限定して上皮系腫瘍 30 症例、非上皮系腫瘍 28 症例、ウイルス感染症 8 症例、その他 5 症例を含む合計 70 症例の病理標本スライドをスキャンした。

C.研究結果

画像容量は合計約 70GB、一症例あたり約 500MB～5GB(対物 X40 でスキャン)、一枚あたりのスキャンにかかる時間は数分であった。バーチャルスライドを用いた講義の利点は①低～高倍率に移動する場合に連続的拡大像を連続的視覚的にとらえられ、病変部以外も随時提示できた。②病変の全体像の理解を高めることができた。③学生の質問にも臨機応変に対応できた。問題点は①繊細な画像を提示する為に対物 X40 でスキャンしたが、画像データの容量が大きくなった。②スキャンやデータ整理に手間がかかった。③限られた講義時間内で多数の症例を提示する必要があり、最小限の病理組織像を効率良くスキャンする必要があり、講義者自らがスキャンする必要があった。

D.考察

上記問題点が改善されていけば、バーチャルスライドが学習ツールとしての普及に繋がると思われた。

E.結論

医学部学生や初期臨床研修医の学習教育、各種専門医医師養成に対しバーチャルスライドは実践的病

理学学習ツールの有用な発展性が期待できる。

F.研究発表

1. 論文発表

1. Ishihara S, Honda Y, Asato T, Nonaka M, Nakagawa S, Hirashima K, Hayashi N, Baba H, Iyama K: Intergigitating dendritic cell sarcoma of the ileum recurred in multiple lymph nodes and duodenum three years after operation without chemotherapy. Path Res Pract. 206: 514-18, 2010.

2. Makino K, Kojima R, Nakamura H, Morioka M, Iyama K, Shigematsu K, Kuratsu J: Ectopic adrenal cortical adenoma in the spnal region:case report and review of the literature. Brain tumor Pathol. 27:121-125, 2010.

3. Mori T, Ohba Y, Shiraishi K, Iwatani K, Yoshimoto K, Iyama K: A case of sclerosing hemangioma evaluated with diffusion-weighted magnetic resornance imaging and 18F-fluorodeoxyglucose positron emission tomography. Ann Thorac Cardiovasc. 16: 276-286, 2010.

2.学会発表

1. 本田由美、猪山賢一：バーチャルスライドを用いた皮膚腫瘍性病変の病理学講義の試み、厚生省がん臨床研究事業 VS 研究班、平成 22 年度第二回班会議,2010.2.10（盛岡市：岩手医科大学）

Pathology – Research and Practice 206 (2010) 514–518

Contents lists available at ScienceDirect

Pathology – Research and Practice

journal homepage: www.elsevier.de/prp

Teaching cases

Interdigitating dendritic cell sarcoma of the ileum recurred in multiple lymph nodes and duodenum three years after operation without chemotherapy

Sonoko Ishihara [a,*], Yumi Honda [a], Tsuguharu Asato [a], Michiyasu Nonaka [b], Shigeki Nakagawa [c], Kotaro Hirashima [c], Naoko Hayashi [c], Hideo Baba [c], Ken-ichi Iyama [a]

[a] Department of Surgical Pathology, Kumamoto University Hospital, 1-1-1 Honjo, Kumamoto 860-8556, Japan
[b] Nishinihon Hospital, Kumamoto, Japan
[c] Department of Gastroenterological Surgery, Faculty of Medical and Pharmaceutical Sciences, Kumamoto University, Kumamoto, Japan

ARTICLE INFO

Article history:
Received 20 October 2009
Received in revised form
11 December 2009
Accepted 17 January 2010

Key words:
Interdigitating dendritic cell sarcoma
Ileum
Lymph node
Duodenum
Chemotherapy

ABSTRACT

Neoplasms derived from interdigitating dendritic cell are extremely rare. Here we describe a case of a 47-year-old man with interdigitating dendritic cell sarcoma (IDCS) in the ileum. He was admitted to a hospital due to ileus. The ileal tumor, measuring 2 cm, was detected and resected with regional lymphadenectomy. At that time, a pathologic diagnosis of malignant peripheral nerve sheath tumor was made. The patient, who was not treated with chemotherapy, showed no signs of recurrence. After three years, we detected cervical lymphadenopathy and multiple duodenal masses in the patient in our hospital. Oval to spindle-shaped atypical cells, which resembled ileal tumor cells, infiltrated into the lymph node and duodenum. Immunohistochemical staining of these three lesions revealed positivity of S100 protein and several macrophage-related antigens. Based on the histologic and immunohistochemical analysis, the histopathologic diagnosis of IDCS was confirmed. To our knowledge, five cases of IDCS arising in the intestinal tract have been reported to date, and only one case, treated with both surgery and chemotherapy, led to remission. This is the first case that has a comparatively favorable prognosis without chemotherapy after surgery.

Introduction

Dendritic cells (DC) are arachnoid immune accessory cells derived from the hematopoietic stem cell. They are composed of several subtypes: Langerhans cells, interdigitating dendritic cells, follicular dendritic cells, dermal dendrocytes, interstitial DC, and veiled cells. Interdigitating dendritic cells are located in T-cell areas in the paracortex and deep cortex of lymph nodes, tonsil, splenic periarteriolar lymphoid sheath, and interfollicular areas of mucosa-associated lymphoid tissue. They are antigen-presenting cells responsible for initiating primary and secondary T-lymphocyte immune responses through major surface histocompatibility complex–peptide complexes [7,10–12,14]. Most of DC sarcomas occur in lymph nodes, and one-third of them involve extranodal sites. Neoplasms arising from interdigitating dendritic cells are uncommon, and 55 cases of interdigitating dendritic cell sarcoma (IDCS) have been reported [13]. The sites of extranodal IDCS are liver (27%), spleen (18%), skin (15%), lung (12%), nasopharynx, small intestine, mesentery, testis, tonsil, bone marrow, chest wall, paraspinal area, bladder, salivary gland, and breast [2,11,13]. In general, IDCS is an aggressive tumor. The median overall duration of survival is 10 months [5,11]. To our knowledge, five cases of IDCS involving the intestine have been reported [1,3,4,8], and only one case, treated with surgery and chemotherapy, was free of disease. Here we describe the first case of IDCS in the ileum in which there has been no sign of recurrence for three years although the patient was not treated with chemotherapy after surgery.

Clinical summary

A 47-year-old male was admitted to a hospital due to right lower abdominal pain. Radiologic examination demonstrated marked dilatation of the small bowel tract (Fig. 1a) and intussusception (Fig. 1b), suggesting ileus. The obstruction could not be resolved despite conservative management. As the cause of intussusception was unknown, an exploratory laparotomy was performed two weeks after admission. During the operation, the ultrasound and endoscopic examination revealed two submucosal

* Corresponding author. Tel./fax: +81-96-373-7097.
E-mail address: snk0211@fc.kuh.kumamoto-u.ac.jp (S. Ishihara).

0344-0338/$ - see front matter © 2010 Elsevier GmbH. All rights reserved.
doi:10.1016/j.prp.2010.01.009

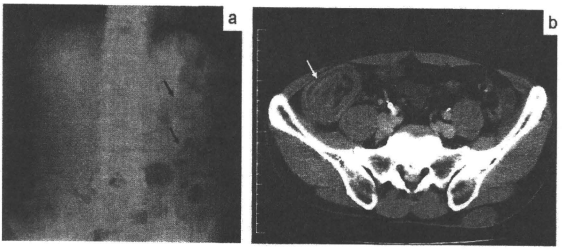

Fig. 1. Radiologic findings: (a) an abdominal X-ray film shows marked intestinal dilatation (arrows) and (b) computed tomography reveals intussusception in the ileum, which leads to target sign (arrow).

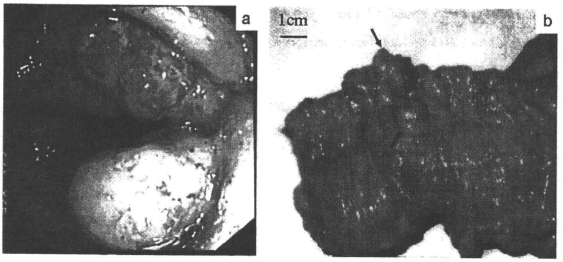

Fig. 2. Macroscopic view of ileal tumor: (a) the endoscopic examination shows elevated tumors with ulceration in the ileum and (b) the tumors are two superficially elevated lesions measuring approximately 1 and 2 cm in size (arrows).

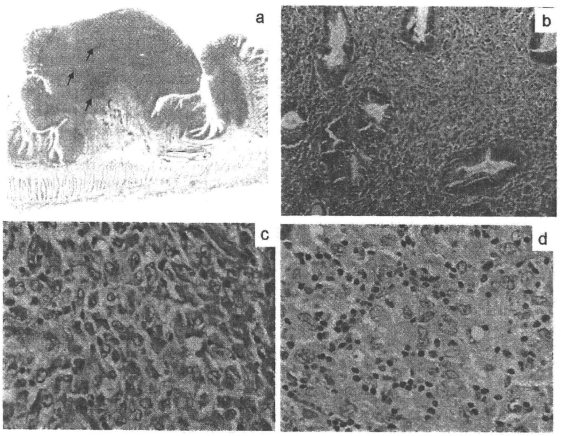

Fig. 3. Histologic findings of the tumor; a, b, and c show the ileal tumor: (a) atypical cells of the primary tumor in the ileum diffusely proliferate in the mucosa and submucosal tissue; Peyer's patch is observed (arrow), (b) in the mucosa, normal gland also remained, (c) the tumor is composed of oval to spindle-shaped cells and (d) biopsy of cervical lymph node. Atypical cells resembling the tumor cells in the primary ileal mass infiltrate diffusely.

tumors in the ileum, about 10 cm away from the ileocecal valve (Fig. 2a). They were found to be superficially elevated tumors. One was 2 cm and the other 1 cm in diameter (Fig. 2b). The patient underwent an ileocecal resection and a right hemicolectomy with regional lymphadenectomy because of enlargement of four lymph nodes around the right ascending colon. The patient was histologically diagnosed as having malignant peripheral nerve sheath tumor. Chemotherapy was not performed, and there was no definite evidence of recurrence. However, three years after the operation, computed tomography revealed multiple lymphadenopathy in the cervix, supraclavicular fossa, mediastinum, and around the abdominal aorta. He was referred to our hospital, and a biopsy from the cervical lymph node was made. Esophagogastroduodenoscopy revealed multiple elevated masses in the duodenum, and a biopsy of the tumor was also made.

Microscopic findings

The tumor cells in the ileum proliferated diffusely in the mucosal and underlying submucosal tissue. Peyer's patch and its remnants were found (Fig. 3a). Normal glands were seen around the tumor cells in the mucosal tissue (Fig. 3b). The tumor cells were of large size and had a lobated, folded nucleus with dispersed chromatin and prominent nucleoli. Their cytoplasm

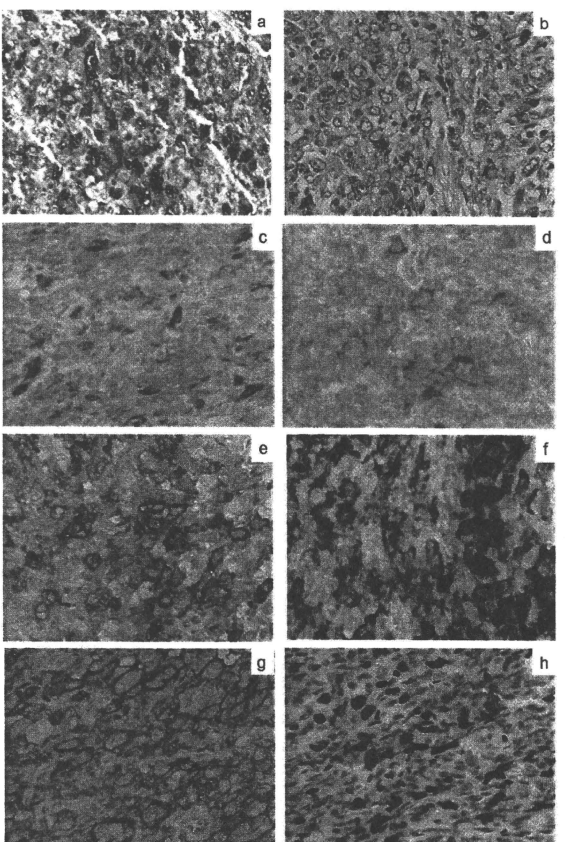

Fig. 4. Immunohistochemical findings of the ileal tumor. The tumor cells demonstrate reactivity for (a) S100 protein, (b) CD68, (c) fascin, (d) CD11c, (e) CD163, (f) CD204, (g) HLA-DR, and (h) the proliferation rate (MIB-1 index) is 10%.

was eosinophilic with an indistinct cell border. Small lymphocytes, plasma cells, and eosinophils infiltrated into the background (Fig. 3c). The mitotic rate is 6 per 10 high-power fields. Tumor cells also infiltrated into all of the resected lymph nodes. Necrosis was not present. Hemophagocytosis by tumor cells was not identified in the affected lymph nodes.

Immunohistochemically, tumor cells in the ileum were diffusely positive for S100 protein in the nucleus and the cytoplasm (Fig. 4a); vimentin in the cytoplasm and CD68 in the cytoplasm and on the cell surface (Fig. 4b) were focally positive. In the cytoplasm, they also focally expressed fascin (Fig. 4c), CD11c (Fig. 4d), CD163 (Fig. 4e), and CD204 (Fig. 4f). There was diffuse expression of HLA-DR (Fig. 4g). Tumor cells were negative for CD1a, CD3, CD20, CD21, CD29, CD79a, CD30, CD34, myeloperoxidase, HMB-45, alpha smooth muscle actin, cytokeratin, lysozyme, EBNA-2, or LMP-1. There was no reactivity with in situ hybridization for Epstein-Barr virus (EBV)-encoded RNAs. The MIB-1 labeling index was 10% (Fig. 4h). The tumor cells of the ileum, cervical lymph node (Fig. 3d), and duodenum shared similar histologic and immunohistochemical features. We did not perform electron-microscopic examination because fresh material could not be prepared.

Discussion

IDCS occurs from 8 to 77 years (a median age of 52 years), with a slight predominance for men. IDCS shows a spectrum of architectural and cytologic morphologies. The neoplastic cells are medium to large in size, and have a spindle to plump shape with indistinct cell borders. They have an oval, central nucleus with finely dispersed chromatin and a prominent nucleolus. Scattered multinucleated cells are often seen. IDCS shows diffuse proliferation with a sinusoidal, nesting, fascicular, and storiform growth pattern. While there is no specific marker for IDCS, immunohistochemical analysis can help in the differentiation from other sarcomas. One of the ultrastructual characteristics of interdigitating dendritic cells is the occurrence of interdigitating cytoplasmic processes on their surface; however, they lack Birbeck granules [2,6,13].

The diagnosis of IDCS is sometimes difficult because DC differentiation cannot be evaluated only on hematoxylin and eosin specimens due to the histologic similarity to other neoplasms. Actually, in our case, hematologic tumors, spindle cell neoplasms, and malignant melanoma were listed as the first differential diagnosis because the tumor cells had ovoid to spindle nuclei and lacked a glandular structure and epithelial morphology. We presume that these tumor cells originated from histiocytic or dendritic cells as they were immunohistochemically stained with S100 protein and macrophage-associated antigen. Moreover, B-cell or T-cell lymphoma, malignant melanoma, or other spindle cell neoplasms could be excluded by the immunohistochemical analysis. Therefore, the second differential diagnosis for this tumor included histiocytic and dendritic cell neoplasms. The additional immunohistochemical analysis revealed that tumor cells were positive for fascin, expressed in follicular and interdigitating dendritic cells [2], and CD1a, CD21, and lysozyme were not expressed. Histiocytic sarcoma is composed of larger cells (over 20 μm in diameter). The expression of S100 protein is weak or focal, and hemophagocytosis occasionally occurs in histiocytic sarcoma. Follicular dendritic cell sarcoma (FDCS) may be confused with IDCS because of the whorled growth pattern of spindle cells. FDCS is positive for CD21. The tumor, derived from Langerhans cells, expresses CD1a. According to WHO [11], our case was consistent with the histopathologic and immunohistochemical phenotype of IDCS.

To our knowledge, five cases of IDCS involving the intestinal tract have been reported to date [1,3,4,8]. The small intestine was the common site, and most of those cases were presented with intestinal obstruction, where the size was greater than 5 cm (Table 1). Histologically, tumor cells were reported to infiltrate from the lamina propria into the muscular layers of the small intestine, and mitotic count was found to be high [3]. Vacuolization in the cytoplasm of the tumor and necrotic foci has also been reported [8]. Our case did not show a high mitotic count, necrosis, or cytoplasmic vacuolization. Immunohistochemical analysis revealed consistent reactivity with IDCS in both our's and the reported cases.

IDCS are treated with surgery, radiation therapy, chemotherapy, and a combination of these therapies. The effect of these treatments varies in each case. In localized IDCS, resection was the

Table 1
Summary of interdigitating dendritic cell sarcoma involving intestinal tract.

Author	Year	Patient age (year)/sex	Symptoms	Site	Size (cm)	Treatment	Outcome
Daum et al.[3]	1985	43/M	Abdominal pain Anorexia	Jejunum	4–5	Resection Chemotherapy	Died of disease
Miettinen et al.[8]	1992	52/F	Intestinal obstruction	Small intestine Retroperitoneum Mediastinum	8	Resection Chemotherapy	Died of disease
	1992	58/M	Abdominal pain Anorexia Vomiting	Terminal ileum Liver nodules	8	Resection Chemotherapy	Free of disease 12-month follow-up
Banner et al.[1]	1996	68/F	Abdominal distention Vomiting	Cecum	8	Resection Chemotherapy	Alive with disease 3-month follow-up
Kanaan et al.[4]	2006	36/F	Epigastric pain Disphagia Vomiting	Duodenum Lymph nodes Liver	Not reported	Resection	Died of disease
Present case		47/M	Abdominal pain	Terminal ileum Lymph nodes Duodenum	2	Resection and chemotherapy after relapse	Free of disease 3-year follow-up and alive with disease 8-month follow-up

curative therapy in more than half of the cases, and chemotherapy performed after surgery did not improve the disease-free survival [12,13]. Most of the advanced IDCS cases, which survived for several years, were treated with chemotherapy and/or radiation therapy [2]. Moreover, a good response to chemotherapy has been reported in an advanced case without surgery [9]. In the reported four cases of IDCS affecting the small intestine, chemotherapy was done following resection, and only one case among them survived without disease. IDCS arising from the duodenum, with liver and peripancreatic lymph node involvement, developed rapidly, and chemotherapy could not be performed (Table 1). Tumors greater than 5 cm, arising from the abdomen, are related to a poorer clinical outcome, and a high mitotic count or the presence of necrosis may be a risk factor indicating an unfavorable prognosis [13]. In the present case, IDCS occurred in the ileum, and regional lymph node metastases were detected. The patient showed no sign of recurrence during the next three years after operation, without chemotherapy or radiation therapy. The small size of the tumor might relate to a comparatively favorable prognosis. After recurrence of IDCS in both the duodenum and the lymph nodes, chemotherapy was partially effective.

In summary, we herein document the first case of advanced IDCS in the ileum. There has been no relapse for three years after surgery, without chemotherapy. IDCS is a rare neoplasm, and extranodal IDCS is more uncommon than nodal IDCS. The final diagnosis was made when the tumor recurred in the multiple lymph nodes and duodenum. As the immunohistochemical analysis of DC markers is not a routine procedure, and there is no specific marker, awareness of the morphologic and immunophenotypic features of such rare neoplasm is important, keeping in mind a differential diagnosis of histiocytic and spindle cell tumors.

Acknowledgments

We are grateful to Drs. Motohiro Takeya and Koji Ohnishi (Department of Cell Pathology, Graduate School of Medical Sciences, Kumamoto University) for their excellent technical assistance in immunohistologic analysis.

References

[1] B. Banner, M.L. Beauchamp, M. Liepman, B.A. Woda, Interdigitating reticulum-cell sarcoma of the intestine: a case report and review of the literature, Diagn. Cytopathol. 17 (1997) 216–222.
[2] E.M. Gaertner, M. Tsokos, G.A. Derringer, T.S. Neuhauser, C. Arciero, J.A. Andriko, Interdigitating dendritic cell sarcoma. A report of four cases and review of the literature, Am. J. Clin. Pathol. 115 (2001) 589–597.
[3] G.S. Daum, M. Liepman, B.A. Woda, Dendritic cell phenotype in localized malignant histiocytosis of the small intestine, Arch. Pathol. Lab. Med. 109 (1985) 647–650.
[4] H. Kanaan, J. Al-Maghrabi, A. Linjawi, A. Al-Abbassi, A. Dandan, A.R. Haider, Interdigitating dendritic cell sarcoma of the duodenum with rapidly fatal course: a case report and review of the literature, Arch. Pathol. Lab. Med. 130 (2006) 205–208.
[5] K. Kawachi, Y. Nakatani, Y. Inayama, N. Kawano, N. Toda, K. Misugi, Interdigitating dendritic cell sarcoma of the spleen: report of a case with a review of the literature, Am. J. Surg. Pathol. 26 (2002) 530–537.
[6] K. Pillay, R. Solomon, J.D. Daubenton, C.C. Sinclair-Smith, Interdigitating dendritic cell sarcoma: a report of four paediatric cases and review of the literature, Histopathology 44 (2004) 283–291.
[7] K. Takahashi, K. Asagoe, J. Zaishun, H. Yanai, T. Yoshino, K. Hayashi, T. Akagi, Heterogeneity of dendritic cells in human superficial lymph node *in vitro* maturation of immature dendritic cells into mature or activated interdigitating reticulum cells, Am. J. Pathol. 153 (1998) 745–755.
[8] M. Miettinen, C.D. Fletcher, J. Lasota, True histiocytic lymphoma of small intestine. Analysis of two S-100 protein-positive cases with features of interdigitating reticulum cell sarcoma, Am. J. Clin. Pathol. 100 (1993) 285–292.
[9] M.J. Oines, T. Nicol, M. Duncan, M. Bohlman, R. Erlich, Interdigitating dendritic cell sarcoma: a rare malignancy responsive to ABVD chemotherapy, Leuk. Lymphoma 43 (2002) 817–821.
[10] S.A. Pileri, T.M. Grogan, N.L. Harris, P. Banks, E. Campo, J.K. Chan, R.D. Favera, G. Delsol, C. De Wolf-Peeters, B. Falini, R.D. Gascoyne, P. Gaulard, K.C. Gatter, P.G. Isaacson, E.S. Jaffe, P. Kluin, D.M. Knowles, D.Y. Mason, S. Mori, H.-K. Müller-Hermelink, M.A. Piris, E. Ralfkiaer, H. Stein, L.-J. Su, R.A. Warnke, L.M. Weiss, Tumours of histiocytes and accessory dendritic cells: an immunohistochemical approach to classification from the International Lymphoma Study Group based on 61 cases, Histopathology 41 (2002) 1–29.
[11] S.H. Swerdlow, E. Campo, N.L. Harris, E.S. Jaffe, S.A. Pileri, H. Stein, J. Thiele (Eds.), World Health Organization Classification of Tumours of Haematopoietic and Lymphoid Tissues, fourth ed., IARC Press, Lyon, 2008.
[12] S. Kairouz, J. Hashash, W. Kabbara, W. Mchayleh, I.A. Tabbara, Dendritic cell neoplasms: an overview, Am. J. Hematol. 82 (2007) 924–928.
[13] T. De Pas, G. Spitaleri, G. Pruneri, G. Curigliano, C. Noberasco, A. Luini, B. Andreoni, T. Alessandro, B. Filippo, Dendritic cell sarcoma: an analytic overview of the literature and presentation of original five cases, Crit. Rev. Oncol. Hematol. 65 (2008) 1–7.
[14] V. Wright-Browne, K.L. McClain, M. Talpaz, N. Ordonez, Z. Estrov, Physiology and pathophysiology of dendritic cells, Hum. Pathol. 28 (1997) 563–579.

Brain Tumor Pathol (2010) 27:121–125
DOI 10.1007/s10014-010-0270-z

CASE REPORT

Keishi Makino · Ryota Kojima · Hideo Nakamura
Motohiro Morioka · Ken-ichi Iyama · Kazuto Shigematsu
Jun-ichi Kuratsu

Ectopic adrenal cortical adenoma in the spinal region: case report and review of the literature

Received: April 19, 2010 / Accepted: May 30, 2010

Abstract Ectopic adrenal cortical neoplasms are extremely rare; few involve the central nervous system (CNS). We report a 17-month-old girl with spinal adrenal cortical neoplasms. She was unable to crawl or stand and was irritable at night. Her appearance was asymmetrical; the right side of her face and her lower right leg were enlarged. In addition, she manifested hyperplasia of the thymus, fibrous hyperplasia of the bladder, and hamartoma in the liver. However, all abnormalities were asymptomatic. Magnetic resonance imaging (MRI) revealed well-circumscribed masses within the dura mater at the T12–L1 and L3–L4 level. Histology disclosed that the lesions were composed of sheets and nests of round and polygonal cells with mostly round regular nuclei; eosinophilic to clear cytoplasm was abundant. Immunohistochemically, the tumor cells were strongly positive for inhibin-alpha, positive for synaptophysin and vimentin, and negative for GFAP, EMA, S-100, NSA, and chromogranin A. In addition, the nuclei stained positive for steroidogenic factor 1 (Ad4BP/SF-1), which is involved in adrenal steroidogenesis. This case confirms the occurrence of adrenocortical adenoma in the CNS. We suggest that this tumor should be considered in the differential diagnosis of CNS tumors.

Key words Ectopic adrenal cortical neoplasms · Spinal cord · Childhood · Central nervous system · Immunohistochemistry

K. Makino (✉) · R. Kojima · H. Nakamura · M. Morioka · J. Kuratsu
Department of Neurosurgery, Faculty of Medical and Pharmaceutical Sciences, Kumamoto University Graduate School, 1-1-1 Honjo, Kumamoto 860-8556, Japan
Tel. +81-96-373-5219; Fax +81-96-371-8064
e-mail: kmakino@fc.kuh.kumamoto-u.ac.jp

K. Iyama
Department of Surgical Pathology, Kumamoto University Hospital, Kumamoto, Japan

K. Shigematsu
Department of Pathology, Japanese Red Cross Nagasaki Atomic Bomb Hospital, Nagasaki, Japan

Introduction

The adrenal gland arises from primordial mesenchyme in the wall of the dorsal coelom adjacent to the dorsal mesentery and urogenital structures.[1,2] Therefore, most ectopic adrenocortical tissue is found along the path of embryonic migration within the urogenital tract. The most common sites include the celiac axis (32%), the broad ligament (23%), the adnexa of the testis (7.5%), and the spermatic cord (3%–8%).[3] Adrenocortical tumors, both benign and malignant, can also arise at ectopic sites, presumably from ectopic adrenal rests.[4,5]

A unique anatomic region for ectopic cortical tumors is the lower spinal region.[6–11] We report an unusual patient with ectopic adrenocortical tumors in the spinal region and several systemic anomalies such as hyperplasia of the thymus, fibrous hyperplasia of the bladder, hamartoma in the liver, and asymmetry of the face and lower extremity.

Case report

The mother of this 17-month-old girl noted that she was unable to crawl or stand and that she was irritable at night. Both parents were healthy and had no history of congenital disease. A cystic region in the liver had been diagnosed on ultrasound performed at 28 weeks of gestation; this region was monitored and found to be enlarging gradually. As the membranes ruptured at 34 weeks of gestation, the infant was delivered by cesarean section. The Apgar score was 8, and her birth weight was 2,306 g. Laboratory examination disclosed anemia and hypoglycemia. Her face and lower extremity were asymmetrical; her right cheek and right lower leg were enlarged. Contrast-enhanced abdominal computed tomography (CT) led us to suspect that the cystic mass in the liver was a hamartoma. At this time, there were no obvious neurological deficits.

She was carefully monitored in our pediatric outpatient department. At 7 months, CT revealed enlargement of the thymus. A specimen obtained by open biopsy yielded a

histological diagnosis of hyperplasia. The cystic mass in the liver gradually decreased under observation. At 15 months, her mother found a soft mass protruding through the urethra. Ultrasound identified a solid mass in the bladder; it was removed through the urethra. The histological diagnosis was fibrous hyperplasia without evidence of malignancy. Subsequently her mother noted the child's inability to crawl or stand up and her irritability at night. On neurological examination there was decreased movement of her lower extremities attributable to back pain. Bowel and bladder dysfunction were noted. On magnetic resonance imaging (MRI) scans, well-circumscribed masses were located within the dura mater at the T12–L1 and the L3–L4 levels. The rostral mass was hypointense on both T_1- and T_2-weighted images with homogeneous enhancement (Fig. 1). The caudal mass was slightly hyperintense on T_1-weighted and very hypointense on T_2-weighted images with faint enhancement, findings suggestive of intratumoral hemorrhage (Fig. 1). The brain, upper spinal cord, abdomen, and specifically the adrenal glands were unremarkable on MRI. Based on the location of the masses and their MRI characteristics, they were thought to be myxopapillary ependymoma. Our preoperative differential diagnosis also included Schwannoma and meningioma.

We performed T2–L4 laminectomy for resection of the masses under spinal cord monitoring. The vertebral level was reconfirmed by X-ray before proceeding with the operation. Upon opening the dura mater and arachnoid membrane, two encapsulated masses were noted (Fig. 2). One mass was yellowish-brown, the other was dark red; they were entirely intradural and extramedullary. The rostral tumor was attached to the conus medullaris and nerve roots but readily separated from these structures. The caudal tumor also attached to the nerve roots and contained an old hematoma. Both tumors were well circumscribed and showed no invasion of surrounding tissue. Gross total resection was successful. The child's postoperative course was uneventful, and she was able to resume activities normal for her age and to stand with support.

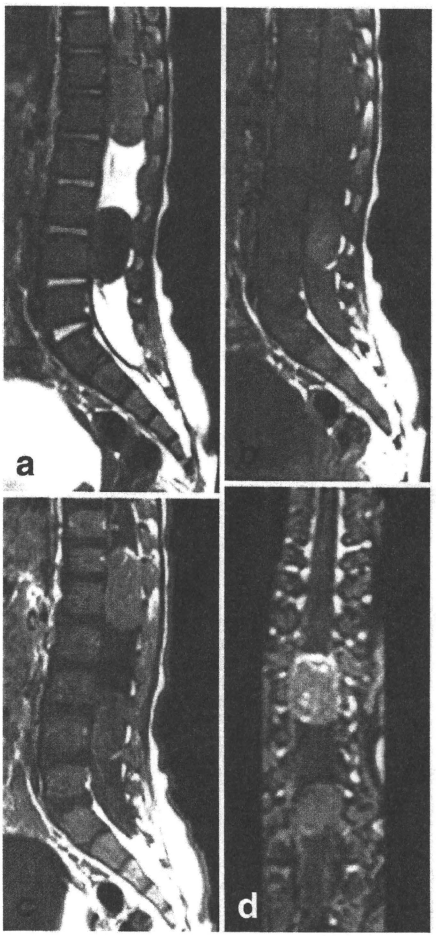

Fig. 1. Magnetic resonance imaging (MRI) revealed well-circumscribed masses at the T12–L1 and the L3–L4 level. The rostral mass was hypointense on both T_2-weighted (**a**) and T_1-weighted (**b**) images with homogeneous enhancement (**c**, **d**). The caudal mass was hypointense on T_2-weighted (**a**) and slightly hyperintense on T_2-weighted (**b**) images with faint enhancement (**c**, **d**)

Pathological findings

Formalin-fixed, paraffin-embedded tissue sections obtained at surgery were submitted for hematoxylin and eosin (H&E) staining and immunohistochemistry. The primary antibodies to synaptophysin (DAKO, 1:50), vimentin (DAKO, 1:400), cytokeratin (NICHIREI, 1:2), CD138 (DAKO, 1:100), CD56 (NOVOCASTRA, 1:50), S-100 (NICHIREI, 1:2), epithelial membrane antigen (EMA) (DAKO, 1:100), chromogranin A (DAKO, 1:100), neuron-specific enolase (NSE) (NICHIREI, 1:2), glial fibrillary acidic protein (GFAP) (DAKO, 1:2500), SF-1 (Ad4BP) (Perseus Proteomics, 15 μg/ml), inhibin-alpha (DAKO, 1:50), and Ki-67/MIB-1 (DAKO,1:50) were used.

Histologically, the specimen was composed of sheets and nests of round and polygonal cells with mostly round regular nuclei and abundant eosinophilic to clear cytoplasm (Fig. 3). Mitoses of 7/20 high-power field (HPF) in the rostral tumor and 4/20 HPF in the caudal tumor were found. The caudal tumor contained hemorrhagic and necrotic foci. Our differential diagnosis included paraganglioma, adrenal cortical carcinoma or adenoma, and oncocytic neoplasm.

Immunohistochemically, the tumor cells were strongly positive for inhibin, positive for synaptophysin and vimentin (Figs. 4a–c, 5a), and focally positive for cytokeratin and CD138. In contrast, they were negative for S-100, EMA, chromogranin A, NSE, and GFAP. The proliferation index for Ki67 (MIB-1) was 15.0% in the rostral and 14.4% in the caudal tumor (Fig. 4d). In addition, the nuclei stained positive for steroidogenic factor 1 (Ad4BP/SF-1) (Fig. 5b), which is involved in adrenal steroidogenesis.

Our findings indicated that the tumor was oncocytic with an immunoprofile of an adrenal cortical adenoma. Although there was some mitotic activity (MIB-1 15.0 and 14.4%), the absence of invasion into surrounding tissues and the patient's clinical history ruled out adrenocortical carcinoma. Follow-up MRI study performed 2 years after resection yielded no evidence of tumor recurrence.

Fig. 2. Operative view of the tumors. Both rostral (*arrowhead*) and caudal masses (*arrow*) were entirely intradural and extramedullary

Discussion

Ectopic adrenocortical tumors in the nervous system are rare; only a few cases have been documented.[6–11] A summary of previously reported cases of spinal adrenocortical adenoma is presented in Table 1. Ectopic adrenocortical tumors in the nervous system seem to locate exclusively in the lower spinal region; the median patient age is 21.5 years, and there is a strong female predominance (7:1). Of eight such tumors, two were intramedullary and the other six, including ours, were intradural and extramedullary.

The MRI features of spinal adrenocortical adenomas are nonspecific; they share signal characteristics with common spinal tumors such as ependymoma, schwannoma, meningioma, and metastasis. According to Harrison et al.[3] they may appear hypo- or hyperintense on T_1-weighted images and slightly hypointense on T_2-weighted images. In our patient the rostral tumor was hypointense on both T_1- and T_2-weighted images and manifested homogeneous enhancement. The appearance of the caudal tumor was affected by intratumoral hemorrhage. In the absence of reports on spinal adrenocortical adenomas with hemorrhage, it was

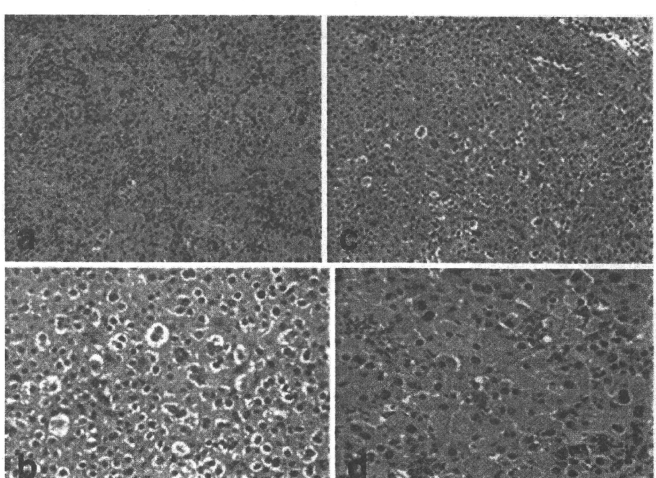

Fig. 3. Hematoxylin and eosin staining of rostral (**a**, **b**) and caudal (**c**, **d**) tumors shows sheets and nests of round and polygonal cells with mostly round regular nuclei and an abundance of eosinophilic to clear cytoplasm at low- and high-power magnification. **a**, **c** ×40; **b**, **d** ×200

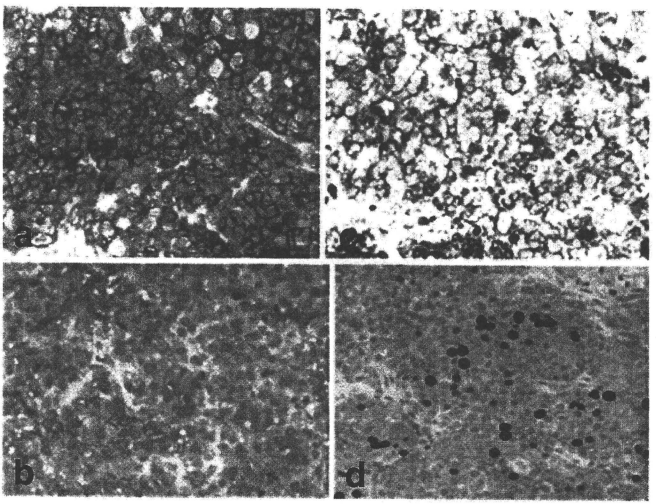

Fig. 4. Immunohistochemical staining of samples from the rostral tumor. The tumor cells were positive for synaptophysin (**a**), inhibin-alpha (**b**), and vimentin (**c**). The proliferation index for Ki67 (MIB-1) was 15% (**d**). **a–c** ×200

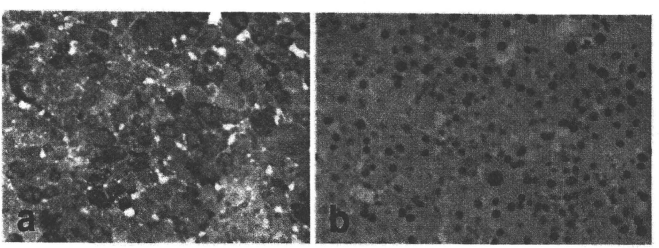

Fig. 5. Immunohistochemical staining of samples from the caudal tumor. The tumor cells were positive for inhibin-alpha (**a**) and steroidogenic factor 1 (SF-1/Ad4BP) (**b**). **a, b** ×200

Table 1. Ectopic spinal adrenocortical adenoma

	Age/sex	Lesion location	Symptoms
Kepes et al.[8]	8 years/F	Extramedullary, L2	Pain
Mitchell et al.[9]	16 years/F	Extramedullary, L2	Pain
	63 years/F	Extramedullary, cauda equina	Pain
Cassarino et al.[6]	27 years/M	Intramedullary, conus medullaris	Weakness, hypoesthesia
Karikari et al.[7]	27 years/F	Intramedullary, L2	Pain
Schittenhelm et al.[10]	44 years/F	Extramedullary, L1	Pain
Rodriguez et al.[11]	5 months/F	Extramedullary, T10–L2	Pain, irritability
Present case	1 year/F	Extramedullary, T12–L1, L3–L4	Pain; bladder and rectal disturbance

difficult to reach a differential diagnosis based on radiologic findings.

Histologically, the differential diagnosis of spinal adrenocortical tumors is broad and includes myxopapillary ependymoma, oncocytic meningioma, and paraganglioma of the filum terminale. Microscopic examination revealed an eosinophilic neoplasm with tumor cells clustered in lobular and nest patterns. In immunohistochemical studies, the positive expression of steroidogenic factor 1 (SF-1/Ad4BP), inhibin-alpha, and synaptophysin has been used to diagnose adrenocortical adenomas. These findings and the negative immunostaining for chromogranin, S-100, EMA, and GFAP led to our diagnosis. Our case lacked the typical features of paraganglioma, i.e., the zellballen archi-

tektur, chromogranin expression, and S-100-positive sustentacular cells. Oncocytic meningiomas express EMA and usually exhibit typical meningothelial features. Myxopapillary ependymoma is characterized by glial cells radiating around vascular structures in papillary configurations within a mucoid stroma. The cells are GFAP positive and should not be immunohistochemically positive for inhibin and SF-1/Ad4BP. The immunohistochemical evaluation for SF-1/Ad4BP, a transcription factor of all steroidogeneses, can aid in rendering a differential diagnosis because nuclear immunoreactivity for this transcriptional factor is relatively specific to steroid-producing cells.[12]

Although the origin of spinal adrenal tumors is not clear, they are thought to derive from ectopic adrenocortical tissue. Adrenal remnants may persist along the embryonic migration path in the spermatic cord, adnexa of testes, groin, and retroperitoneal space.[13,14] Karikari et al.,[7] who encountered a case associated with a tethered cord and lipoma, speculated that premature separation of ectoderm from neuroectoderm before the completion of neurulation permits invasion of the neural groove by mesodermal tissue committed to the formation of adrenocortical tissue. In extramedullary adrenocortical tumors lacking an association with dysraphism, retroperitoneal adrenal rests gaining intradural access by way of exiting nerves or entering vessels has been postulated.[8]

Our case is unique in that it featured several abnormalities including asymmetry of the face and lower extremity, hyperplasia of the thymus, hamartoma in the liver, and fibrous hyperplasia in the bladder. These findings suggest some genetic abnormality, although there was no significant family history of malignant diseases.

Our understanding of molecular alterations underlying the pathogenesis of adrenocortical tumors has been advanced by high-throughput molecular techniques.[15-19] Comparative genomic hybridization showed that aberrations in chromosomes 1p, 4q, 5, 11, 12, and 17 are common in individuals with these neoplasms. Sidhu et al.[18] reported that specifically gains in chromosomes 5 and 12 and losses in chromosome regions 1p and 17p are more closely associated with carcinoma than adenoma. Furthermore, loss of heterozygosity at 9p21, the locus for the tumor suppressor gene p16, is more frequent in adrenocortical carcinomas than adenomas.[20] Studies are under way in our laboratory to examine genetic aberrations in our patients to gain a better understanding of the pathogenesis of her tumors.

In summary, we reported a primary adrenocortical adenoma in the spinal regions of an infant. Gross total resection appeared to be curative. Immunohistochemical studies that include inhibin-alpha, synaptophysin, S-100, chromogranin, and SF-1/Ad4BP were useful in the rendering of an accurate diagnosis.

References

1. Lack EE (1998) Adrenal cortex. In: Kovacs K, Asa SL (eds) Functional endocrine pathology. Blackwell Science, Malden, pp 596–636
2. Skandalakis JE, Gray SW, Scaljon WM, et al (1994) The suprarenal glands. In: Skandalakis JE, Gray SW (eds) Embryology for surgeons. William & Wilkins, Baltimore, pp 718–735
3. Harrison LA, McMillan JH, Batnitzky S, et al (1990) MR appearance of an ectopic intraspinal adrenal cortical adenoma. AJNR Am J Neuroradiol 11:185–1187
4. Wallace EZ, Leonidas JR, Stanek AE, et al (1981) Endocrine studies in a patient with functioning adrenal rest tumor of the liver. Am J Med 70:1122–1125
5. Morimoto Y, Hiwada K, Nanahoshi M, et al (1971) Cushing's syndrome caused by malignant tumor in the scrotum: clinical, pathologic and biochemical studies. J Clin Endocrinol Metab 32:201–210
6. Cassarino DS, Santi M, Arruda A, et al (2004) Spinal adrenal cortical adenoma with oncocytic features: report of the first intramedullary case and review of the literature. Int J Surg Pathol 12:259–264
7. Karikari IO, Uschold TD, Selznick LA, et al (2006) Primary spinal intramedullary adrenal cortical adenoma associated with spinal dysraphism: case report. Neurosurgery 59:E1144; discussion E1144
8. Kepes JJ, O'Boynick P, Jones S, et al (1990) Adrenal cortical adenoma in the spinal canal of an 8-year-old girl. Am J Surg Pathol 14:481–484
9. Mitchell A, Scheithauer BW, Sasano H, et al (1993) Symptomatic intradural adrenal adenoma of the spinal nerve root: report of two cases. Neurosurgery 32:658–661; discussion 661–652
10. Schittenhelm J, Ebner FH, Harter P, et al (2009) Symptomatic intraspinal oncocytic adrenocortical adenoma. Endocr Pathol 20:73–77
11. Rodriguez FJ, Scheithauer BW, Erickson LA, et al (2009) Ectopic low-grade adrenocortical carcinoma in the spinal region: immunohistochemical and molecular cytogenetic study of a pediatric case. Am J Surg Pathol 33:142–148
12. Sasano H, Suzuki T, Moriya T (2006) Recent advances in histopathology and immunohistochemistry of adrenocortical carcinoma. Endocr Pathol 17:345–354
13. Barwick TD, Malhotra A, Webb JA, et al (2005) Embryology of the adrenal glands and its relevance to diagnostic imaging. Clin Radiol 60:953–959
14. Mares AJ, Shkolnik A, Sacks M, et al (1980) Aberrant (ectopic) adrenocortical tissue along the spermatic cord. J Pediatr Surg 15:289–292
15. Gicquel C, Bertagna X, Gaston V, et al (2001) Molecular markers and long-term recurrences in a large cohort of patients with sporadic adrenocortical tumors. Cancer Res 61:6762–6767
16. Kjellman M, Kallioniemi OP, Karhu R, et al (1996) Genetic aberrations in adrenocortical tumors detected using comparative genomic hybridization correlate with tumor size and malignancy. Cancer Res 56:4219–4223
17. Sidhu S, Gicquel C, Bambach CP, et al (2003) Clinical and molecular aspects of adrenocortical tumourigenesis. A N Z J Surg 73:727–738
18. Sidhu S, Marsh DJ, Theodosopoulos G, et al (2002) Comparative genomic hybridization analysis of adrenocortical tumors. J Clin Endocrinol Metab 87:3467–3474
19. Slater EP, Diehl SM, Langer P, et al (2006) Analysis by cDNA microarrays of gene expression patterns of human adrenocortical tumors. Eur J Endocrinol 154:587–598
20. Pilon C, Pistorello M, Moscon A, et al (1999) Inactivation of the p16 tumor suppressor gene in adrenocortical tumors. J Clin Endocrinol Metab 84:2776–2779

Case Report

A Case of Sclerosing Hemangioma Evaluated with Diffusion-Weighted Magnetic Resonance Imaging and ^{18}F-Fluorodeoxyglucose Positron Emission Tomography

Takeshi Mori, MD, PhD,[1] Yasuomi Ohba, MD,[1] Kenji Shiraishi, MD, PhD,[1] Kazunori Iwatani, MD,[1] Kentaro Yoshimoto, MD,[1] and Ken-ichi Iyama, MD, PhD[2]

A 33-year-old female patient was referred to our hospital for further examination of an abnormal shadow evident on a chest X-ray film. Chest computed tomography (CT) revealed a solid nodule 1.9 cm in diameter in the hilum of the upper lobe of the left lung. Positron emission tomography showed high ^{18}F-fluorodeoxyglucose accumulation in the nodule with a maximal standardized uptake value of 4.5, which favored a malignant lesion. Diffusion-weighted magnetic resonance imaging (DWI), which shows differences in the diffusion of water molecules and can discriminate between malignant and benign lesions, indicated that the nodule had a minimum apparent diffusion coefficient of 1.7×10^{-3} mm^2/sec, which was higher than the cutoff value of 1.1×10^{-3} mm^2/sec for discriminating between malignant and benign diseases; i.e., values equal to or lower than 1.1×10^{-3} mm^2/sec favor malignant disease. The results of a CT-guided needle biopsy of the nodule favored sclerosing hemangioma. During surgery, the tumor did not appear to be invasive, and lymph node metastasis and dissemination were not apparent. On the basis of gross appearance, location, preoperative histological diagnosis, and DWI findings, the tumor was enucleated from the pulmonary parenchyma. Seven months after surgery, the patient was alive and had no evidence of recurrent disease. (Ann Thorac Cardiovasc Surg 2010; 16: 276–280)

Key words: sclerosing hemangioma, ^{18}F-fluorodeoxyglucose positron emission tomography, diffusion-weighted magnetic resonance imaging

Introduction

Sclerosing hemangioma is a rare lung tumor thought to derive from primitive respiratory epithelium,[1,2] as first reported by Liebow and Hubell in 1956.[3] Although one case with recurrence[4] and several with hilar or mediastinal lymph node involvement[2,5–9] have been reported, no deaths associated with this disorder have been reported.[2]

In recent years, positron emission tomography (PET) using ^{18}F-fluorodeoxyglucose (FDG) has been successfully used to discriminate malignant from benign pulmonary nodules.[10–12] However, FDG-PET has been reported to give false-positive results in some cases of sclerosing hemangioma,[13,14] which adversely affects the ability to discriminate between benign and malignant nodules and to develop an appropriate therapeutic strategy.

Recent developments in magnetic resonance (MR) gradient technology have enabled the acquisition of diffusion-weighted MR imaging (DWI), which provides excellent tissue contrast based on differences in the diffusion of water molecules among tissues[15–17] and is different from ordinary T_1- and T_2-weighted images. Because the diffusion of water molecules is disturbed by intracellular

From [1]Department of Thoracic Surgery, Graduate School of Medical Sciences, and [2]Division of Surgical Pathology, Kumamoto University Hospital, Kumamoto University, Kumamoto, Japan

Received April 6, 2009; accepted for publication July 6, 2009
Address reprint requests to Takeshi Mori, MD, PhD: Department of Thoracic Surgery, Graduate School of Medical Sciences, Kumamoto University, Honjo 1–1–1, Kumamoto 860–8556, Japan.